

ECOGRAPHY

Research article

An invasive pathogen generally contracts species to their niche cores, not margins

Ben C. Scheele¹✉, Geoffrey W. Heard¹, Richard P. Duncan², Simon Clulow² and Jarrod Sopniewski^{1,3}

¹Fenner School of Environment and Society, Australian National University, Canberra, ACT, Australia

²Center for Conservation Ecology and Genomics, University of Canberra, Canberra, ACT, Australia

³School of Biological Sciences, University of Western Australia, Crawley, WA, Australia

Correspondence: Ben C. Scheele (Ben.Scheele@anu.edu.au)

Ecography

2025: e07612

doi: [10.1111/ecog.07612](https://doi.org/10.1111/ecog.07612)

Subject Editor:

Michael Ray Kearney

Editor-in-Chief:

Christine N. Meynard

Accepted 6 December 2024



Quantifying how species' distributions contract in response to threats can reveal pathways of decline and the role of environmental conditions in moderating threat impacts. Two general patterns of niche contraction have been described: ecological marginalization, where species contract away from threat impacts to peripheral, sub-optimal areas of their niche, and; contraction to the core, where species contract toward their niche center where their fitness and capacity to withstand threat impacts is highest. Recent work has described widespread ecological marginalization in declining mammal species, for which land use change and overexploitation are key threats. Different threatening processes could result in contrasting patterns of niche contraction, although this has not been well-studied. Here, we examine patterns of realized niche contraction in Australian frog species impacted by the emergence of chytrid fungus *Batrachochytrium dendrobatidis*, a pathogen that has driven catastrophic amphibian declines globally. We quantified changes in species' environmental niche space following chytrid emergence and documented a pattern of contraction toward the niche core in declining species. We develop and apply a novel approach to show that these niche contractions are driven by losses in a subset of niche space, suggesting population extinctions due to chytrid are driven by factors shaping both pathogen fitness (threat impact) and host fitness (threat tolerance). Species declines have been concentrated in high elevation areas with cooler temperatures, which are more physiologically suitable for the pathogen and constrain the resilience of frog hosts at both individual and population levels. Given the contrast between our results and widespread ecological marginalization in mammals, we propose that while a given threat may result in common patterns of decline among affected species, patterns of decline may vary considerably between threatening processes and among taxa.

Keywords: chytrid fungus, frog, niche, niche contraction, range



www.ecography.org

© 2025 The Author(s). Ecography published by John Wiley & Sons Ltd on behalf of Nordic Society Oikos

This is an open access article under the terms of the Creative Commons Attribution License, which permits use, distribution and reproduction in any medium, provided the original work is properly cited.

Introduction

In an era when up to 1 million species are at risk of extinction (IPBES 2019) and funding is insufficient to determine all species' responses to threatening processes (Wintle et al. 2019, Eberhard et al. 2022), identifying commonalities in the pathways that species take toward extinction can help identify at-risk taxa and inform conservation prioritization (Britnell et al. 2023, Lomolino 2023). Quantifying patterns of species declines over large spatial and temporal scales is informative in this regard, aided by recent advances in species distribution modelling and widespread digitization of species occurrence records (Lomolino 2023). Conservation biogeography has emerged as a sub-discipline explicitly dedicated to these macroecological patterns of decline and the processes that give rise to them (Richardson and Whittaker 2010). It seeks to inform protected area design, land-use prioritization, and programs focused on species re-introduction, assisted migration and invasive species control (Lomolino 2023).

Of major interest are patterns of species decline in geographic and realized niche space. Two major hypotheses have been proposed, based on two broad patterns of decline. The 'demographic hypothesis' (Lomolino and Channell 1995, Channell and Lomolino 2000a, b) posits that optimal conditions at the range center and niche core allow species to maintain higher population growth rates and abundance (Martínez-Meyer et al. 2013, Pironon et al. 2017, Osorio-Olvera et al. 2020, Fristoe et al. 2023), conferring greater resilience to threats (Hengeveld and Haeck 1982) and resulting in a pattern of contraction to the core. Extensive empirical work has generally supported the pattern of increased abundance closer to the niche core, which sometimes (but not always) corresponds with the center of species geographic ranges (Fristoe et al. 2023). However, contrary to the predictions of the demographic hypothesis, initial efforts to quantify geographic patterns of decline revealed many species were more likely to persist at the geographic margins of their ranges (Lomolino and Channell 1995, Channell and Lomolino 2000a, b). This led Channell and Lomolino (2000a) to propose the 'contagion hypothesis', which postulated that remnant populations of declining species that "persist the longest are those last affected by the contagion-like spread of extinction forces". The contagion hypothesis posits that patterns of species decline are predominantly determined by the pattern of threat emergence and spread, over-riding the expectations of the demographic hypothesis and leading to geographic and/or ecological marginalization. Recent work by Britnell et al. (2023) provides further support for the contagion hypothesis, reporting that declining mammal species commonly underwent ecological marginalization, contracting to the periphery of their ecological niche space. This is concerning, as ecological marginalization may confine species to sub-optimal conditions, potentially increasing the risk of further declines and vulnerability to demographic and environmental stochasticity (Britnell et al. 2023, Lomolino 2023).

However, the generality of ecological marginalization among declining species remains unknown. Existing niche-based analyses of patterns of species decline have focused on mammals (Britnell et al. 2023), for which the most prevalent threats are land use change and over-exploitation (Maxwell et al. 2016, Bogoni et al. 2022). A high prevalence of ecological marginalization is expected in these cases, because habitat loss, habitat degradation and over-exploitation are concentrated in productive, lowland regions that typically support higher numbers of species (Fisher 2011, Watson 2011, Yamaura et al. 2011, Britnell et al. 2023). However, other key threats to biodiversity, such as invasive species and pathogens (Doherty et al. 2016, Maxwell et al. 2016), are not necessarily affiliated with productive lowland areas and could therefore drive contrasting patterns of species niche contraction.

Here, we examine patterns of realized niche contraction in declining frog species impacted by an emerging pathogen, the amphibian chytrid fungus *Batrachochytrium dendrobatidis* (hereafter 'chytrid fungus'). In susceptible species, chytrid fungus results in the disease chytridiomycosis, which is a major driver of amphibian declines globally (Scheele et al. 2019b, Luedtke et al. 2023). We focus on Australian frog species, for which the emergence of chytrid fungus in the late 1970s has been linked with declines in ~20% of species (Scheele et al. 2017b). We have previously shown that the niches of Australian frogs impacted by chytrid fungus contract toward areas with higher temperatures, lower diurnal temperature range, higher precipitation, and lower elevations (Scheele et al. 2023). Here, we examine whether this directional shift has pushed declining frog species to their niche cores or margins.

Patterns of niche contraction in frog species affected by chytrid fungus are likely shaped by the relative performance of the pathogen and hosts across environmental gradients (Nowakowski et al. 2016, Cohen et al. 2017, Scheele et al. 2019a, 2023, Fisher and Garner 2020, Brannelly et al. 2021). Contraction is more likely in environments where pathogen performance is high relative to host performance. Consequently, both contraction to the niche core or ecological marginalization are plausible outcomes for frogs afflicted by chytridiomycosis, depending on the degree of performance overlap between pathogen and host. For example, chytrid fungus is relatively cool adapted, performing best at temperatures in the range of 17–23°C and unable to survive at temperatures above ~28°C (Piotrowski et al. 2004, Sheets et al. 2021). Frog species whose niche core coincides with chytrid's thermal optimum may suffer contractions away from the core toward the warmer margins of their niche where pathogen performance declines to a greater extent than that of the host (Nowakowski et al. 2016, Cohen et al. 2017). In contrast, frog species adapted to conditions much warmer than chytrid's thermal optimum may contract to their core due to losses from their cooler niche margins, coinciding with sites of high pathogen performance and potentially lower host performance (Morrison and Hero 2003). We aimed to evaluate the alternate hypotheses of contraction to the niche core

versus ecological marginalization for Australian frogs affected by chytrid fungus. In doing so, we sought to broaden our understanding of how invasive pathogens alter niche occupancy in declining species.

Material and methods

Species occurrence records

In Australia, chytrid-associated amphibian declines have occurred throughout the eastern seaboard and adjacent ranges, including the island of Tasmania (latitudinal range 12–42°S) (Scheele et al. 2017b). We therefore focused on frog species in this region. Specifically, we included species in three groups: 1) chytrid-threatened ($n=15$), (2) chytrid-nonthreatened ($n=11$), and (3) nonthreatened ($n=22$). The first two groups comprise species with documented chytrid-associated declines as described in Scheele et al. (2017b), with the first group containing species recognized as threatened by the International Union for Conservation of Nature (IUCN), or species recommended for listing as threatened in the review by Gillespie et al. (2020). The second group contains species that experienced less severe declines due to chytrid and are not listed as threatened. The third group of species are congeners that occur in sympatry with species in the two chytrid-impacted groups, but which are not listed as threatened and are not known to have undergone chytrid-related declines. This third group of species was included as a reference point for the two chytrid-impacted groups, given the potential for systematic shifts in sampling effort or other unaccounted factors that could alter observed frog distributions over time.

The acquisition, filtering and expert checking of species occurrence records is described in Scheele et al. (2023). Briefly, we obtained all available occurrence records across eastern Australia from museums, government collections and online repositories. We filtered all records to exclude those with incorrectly coded coordinates (e.g. records in the ocean) or those with latitude and longitude recorded to less than two decimal places. We then removed records outside the known distribution of each species (with a buffer) that were unlikely to be valid (for details see Scheele et al. 2023). The remaining records for each species were examined by species experts to identify and remove likely spurious records. We excluded a small number of records of *Litoria fallax* and *L. gracilentia* in southern Australia that were established by recent human introductions well-beyond their natural range. Due to taxonomic splits for some species since the emergence of chytrid fungus, records from several sister-species were combined (Supporting information). Records were thinned for each species by overlaying a 30-arcsecond grid across Australia and retaining only one record per species in each grid cell.

We identified the estimated year of chytrid emergence for each species using regional reconstructions of the timing of chytrid emergence and subsequent frog declines in eastern Australia as described in Scheele et al. (2017b). The three

regions were the central Eastern Seaboard, north of Sydney, NSW (between ~ 34 and 20°S ; chytrid emergence ~ 1983), southern NSW/Victoria/Tasmania (south of $\sim 34^\circ\text{S}$; chytrid emergence ~ 1985), and Northern Queensland/Wet Tropics (north of $\sim 20^\circ\text{S}$; chytrid emergence ~ 1993). Each species was assigned to the region where the majority of its occurrence records were located. We aimed to compare niche attributes prior to and after chytrid emergence in each of the three species groups. To do this, we assumed the total set of occurrence records captured the full historical distribution of each species, with post-chytrid occurrence records representing the distribution following emergence of the pathogen (Scheele et al. 2023). We refer to these as the ‘full’ and ‘post-chytrid’ distributions hereafter.

Niche hypervolume construction and calculating Mahalanobis distances

We refer to species realized niches as the multidimensional set of environmental and biotic factors that determine the observed geographic distribution of species through their influence on population growth rates (Colwell and Rangel 2009, Peterson et al. 2011). We used multidimensional realized niche hypervolumes to characterize the environmental conditions occupied by species, with the niche centroid defined as the ‘mean realized-niche position in n -dimensional space’ (Guisan et al. 2014).

For each species, a niche hypervolume was constructed using the ‘Hypervolume’ package in R (Blonder et al. 2014, 2018). The environmental variables used were ‘annual mean temperature’, ‘mean diurnal temperature range’, ‘annual precipitation’ and ‘elevation’ obtained from WorldClim 2.0 (Fick and Hijmans 2017) at 30-arcsecond resolution (see Scheele et al. 2023 for rationale and further details). To check for collinearity amongst variables, we calculated the variance inflation factor (VIF) for each variable in the study region (the Australian continent, east of 141° longitude), using the ‘usdm’ package in R (Naimi et al. 2014). The VIF for each variable was < 3 (annual mean temperature, 1.63; mean diurnal range, 2.85; annual precipitation, 2.65; elevation, 1.43), indicating relatively low multicollinearity.

To construct each hypervolume, we extracted the value of each environmental variable associated with each species’ occurrence records using the ‘terra’ package in R (Hijmans et al. 2022), then scaled and centered these values. For species with at least 55 unique records remaining after removing occurrence records with missing information (the recommended number of data points to construct a hypervolume in four-dimensions), we created a niche hypervolume using the support vector machine method, specifying parameters of $\nu=0.01$ and $\gamma=2.5$, following Blonder et al. (2014) and Blonder et al. (2018). To account for the stochastic nature of the hypervolume algorithm, we constructed ten hypervolumes for each species using all occurrence records (assumed full distribution) and a further ten hypervolumes using only the subset of records collected after the chytrid emergence year for each species (post-chytrid distribution).

We then estimated the environmental distance of each occurrence record from the niche centroid by calculating its Mahalanobis distance. Mahalanobis distances are an appropriate measure for multidimensional environmental space as they account for the covariance of multiple environmental axes (Osorio-Olvera et al. 2019, Britnell et al. 2023). For each hypervolume replicate, we first extracted the niche centroid using *get_centroid* from the ‘Hypervolume’ package, then calculated the Mahalanobis distance of each occurrence record to this centroid using the *mahalanobis* function in the base R ‘stats’ package. To facilitate comparisons, we scaled these distances to range between 0 and 1. Finally, to quantify whether each species tended to contract toward its niche core or periphery, we calculated the mean Mahalanobis distance for the post-chytrid occurrence records and subtracted the mean Mahalanobis distance of all records, as in Britnell et al. (2023). For each species, this process was conducted for each of the 10 hypervolume replicates and then averaged. We call this average value ΔMD : it measures by how much the occurrence records have shifted toward or away from the full niche centroid following chytrid emergence. Negative values indicate that, on average, post-chytrid occurrence records are closer to the niche centroid than the full set of occurrence records (contraction to the core), while positive values indicate a shift away from the niche centroid (marginalization). Values around 0 indicate either no niche contraction, or contraction in both core and marginal areas. We tested for differences in ΔMD between species groups (chytrid-threatened, chytrid-nonthreatened and nonthreatened) using a Kruskal–Wallis test in R, with a post hoc Dunn’s test for pairwise comparisons.

To assess the robustness of our results to the method of niche construction employed, we also constructed niche models for each species using a kernel density estimator (KDE), following Broennimann et al. (2021). First, using the same four climatic variables as for the hypervolume method, we performed a principal component analysis for each species using *princomp* in the base R ‘stats’ package, and selected the first two principal components (PCs). On average, these two PCs explained 85.4% (SD 6.0%) of the variation among the four variables. Using a kernel density estimator from the ‘ks’ R package (Duong 2007), we delineated the boundary of each species’ niche by estimating the contour lines corresponding to 99% of the estimated occurrence density along these two PC axes. We then converted each of these delineated niche boundaries to spatial polygons and calculated their centroids using *centroids* from the ‘terra’ package. For each species, we calculated the Mahalanobis distance of each occurrence record to the centroid, as we did for niches constructed using the ‘Hypervolume’ package. The KDE niche construction method also allowed us to calculate the niche margin index (NMI) for each occurrence record as described in Broennimann et al. (2021), which can be used as a complementary measure to characterize niche contractions. The NMI is the minimum distance of each occurrence record to the delineated niche margin; in this case, lower values

indicate records are closer to the margin of the species’ niche. In our analysis, positive values for changes in NMI between the full and post-chytrid occurrence records indicate contraction to the core. Further, to examine the sensitivity of our results to the environmental data used, we re-ran all analyses with data drawn from the CHELSA database (Karger et al. 2023) in addition to our models built using the WorldClim 2.0 database (Fick and Hijmans 2017). We found a high level of congruence in the results produced using both niche construction methods (hypervolume and KDE), the two different climate databases (WorldClim 2.0 and CHELSA), and the different measures of marginalization (Mahalanobis distances versus NMI) (Supporting information). In the main text, we present only the niche hypervolume and WorldClim 2.0 results.

Assessing the uniformity of niche contractions

By calculating ΔMD , we obtain a measure of the overall degree to which each species has contracted toward the margin or core of its niche space. However, this does not provide information on the uniformity of contractions in niche space. For example, a pattern of contraction to the niche center could result from either uniform contraction from all peripheral areas (e.g. a species could contract from both warmer and cooler extremes of their niche) or non-uniform contractions from only certain portions of the niche periphery (e.g. a species contracts from cooler areas whilst persisting in the warmer extremes of their niche). Given that Australian frogs show directional niche contractions post-chytrid (Scheele et al. 2023), we anticipated a non-uniform pattern of contraction.

We quantified the uniformity of contractions by standardizing the loss of niche space in a two-dimensional plane. For each species, we used each of the 10 replicate pairs of full and post-chytrid hypervolumes to assess the uniformity of niche contraction. First, for each pair of environmental variables (six in total, as our hypervolumes were constructed in four dimensions), we extracted the full and post-chytrid centroids (e.g. the centroid for annual mean temperature versus precipitation). In most cases, whether due to actual shifts or the stochastic nature of the hypervolume calculation, these centroids were slightly different. We then calculated the angle between the full and post-chytrid centroids in their actual position, and the position they would hold if the niche had experienced a shift along the x-axis, with the full centroid at $-x$ and the post-chytrid centroid at $+x$ (Fig. 1). The purpose of this was to ‘standardize’ niche shifts to be unidirectional across all environmental pairs. For each occurrence record, we then applied the angular transformation calculated previously such that each record occurred on the adjusted cartesian plane, with points retaining the same distance from the centroid they originally held (Fig. 1). This process was repeated for each of the six pairwise combinations of environmental variables and ten replicates. Hence, in all cases, the post-chytrid niche shift occurred along the x-axis, in the direction of $-x$ to $+x$. Because these adjusted occurrence records now

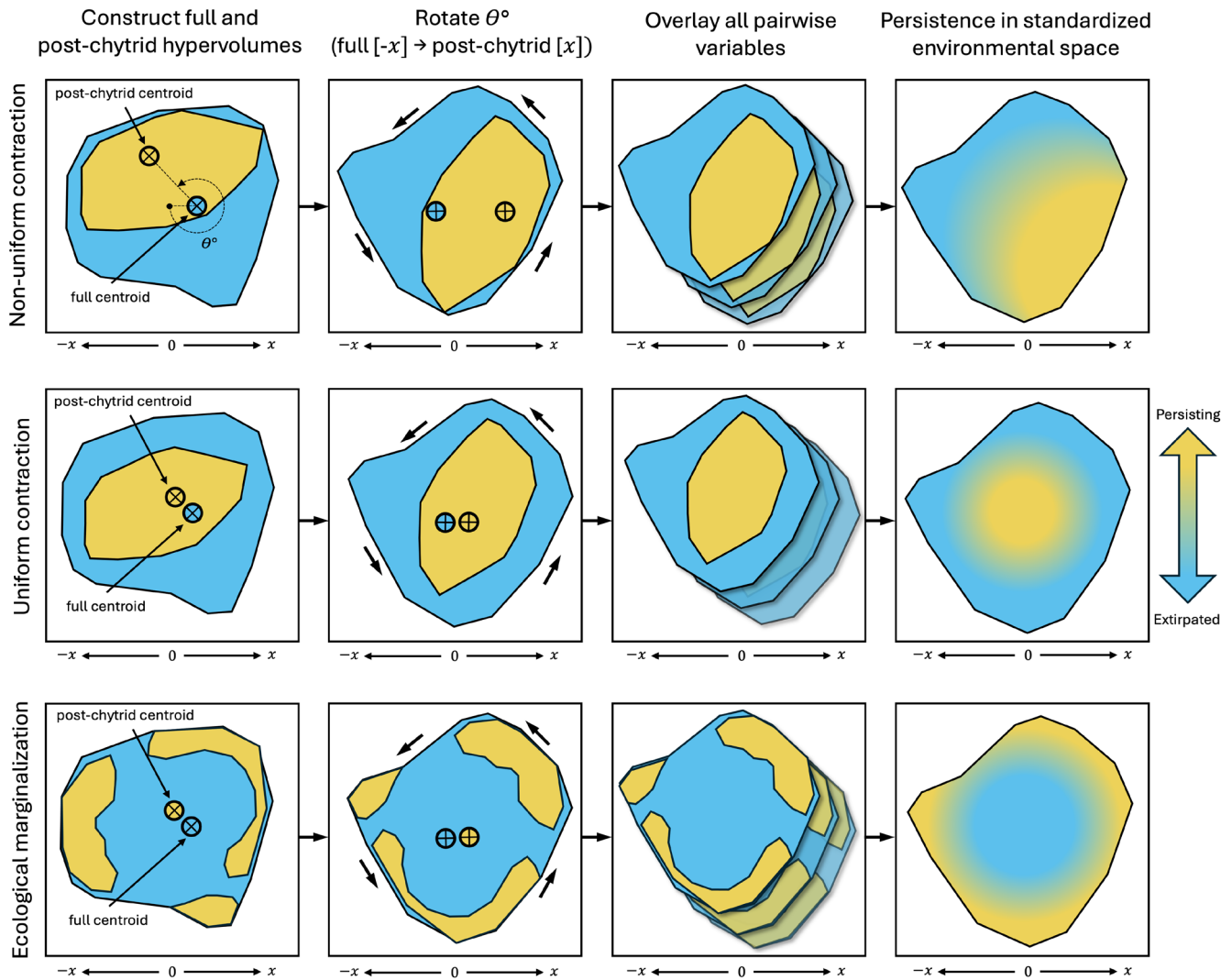


Figure 1. Conceptual representation of the method used to examine the uniformity of species' niche contractions. Each row represents a hypothetical pattern of species niche contraction with the steps used to quantify the uniformity of contraction. In the first two columns, blue shading shows the niche space occupied prior to chytrid emergence (full) while yellow shading shows the niche space occupied after chytrid emergence (post-chytrid). The process shown in each row was completed for all six pairwise combinations of environmental variables, allowing occurrence records to be stacked in a common 2D niche space (third column). The probability of persistence across the full niche space could then be estimated from the distribution of post-chytrid occurrence records relative to the full set of occurrence records (as shown in the final column).

occupied a common 2D niche space, the results for each of the pairwise combinations could be stacked, with the x and y axes representing standardized environmental gradients. For species that experienced non-uniform niche contractions across all pairwise combinations, we should see contraction from the $-x$ direction in all cases. For species that experienced uniform niche contraction, we should see contractions from both the $-x$ and $+x$ directions (Fig. 1).

With species occurrence records plotted in a common 2D niche space, we compared patterns of niche contraction among the three species groups: chytrid-threatened, chytrid-nonthreatened and nonthreatened. For each species, we coded each occurrence record in the full set as either 1 (observed

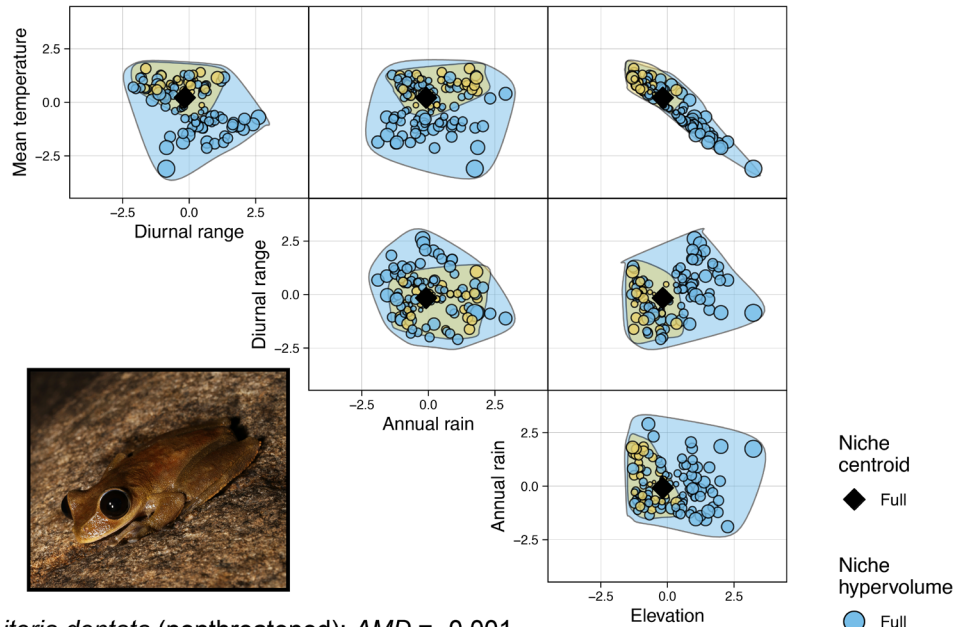
post-chytrid) or 0 (observed pre-chytrid). Assuming post-chytrid records represented persistence (as above), we estimated the probability of persistence post-chytrid across the 2D surface by fitting logistic regression models with the binary response variable and quadratic terms for the coordinates of each occurrence record in the standardized 2D space as predictors. We used the fitted models to predict persistence probability across the surface and then stacked the persistence probabilities for each species in each group, averaging these to obtain the mean probability of persistence across the 2D space. This allowed us to visualize and compare the magnitude and patterns of niche contraction in each species group. Models were fitted in *R* using the base *glm* function.

Results

We constructed niche hypervolumes for 48 Australian frog species and calculated the Mahalanobis distance of each occurrence record from the full niche centroid. We then

calculated the shift in Mahalanobis distance post-chytrid for each species (ΔMD) by subtracting the average Mahalanobis distance of the full set of occurrence records from the average Mahalanobis distance of the post-chytrid occurrence records. **Figure 2** shows two exemplar species, depicting Mahalanobis

Litoria dayi (chytrid-threatened): $\Delta MD = -0.050$



Litoria dentata (nonthreatened): $\Delta MD = -0.001$

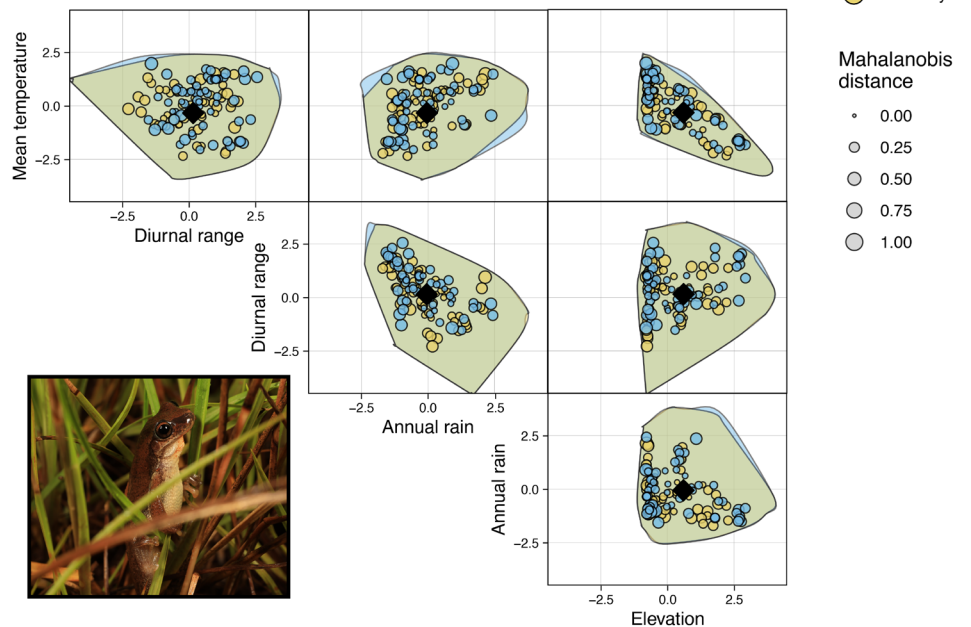


Figure 2. Pairwise plots for the four-dimensional niche hypervolumes showing Mahalanobis distance values, with centroids depicted by tessellated diamonds. The two species illustrate contrasting patterns. The first species, *Litoria dayi*, has experienced a large decline in average Mahalanobis distances post-chytrid, reflecting contraction to the niche core. The pattern of niche contraction is non-uniform with losses concentrated at high elevation and areas with low mean annual temperature. The second species, *L. dentata*, exhibits niche stability with no substantial change in average Mahalanobis distances post-chytrid. For both species, polygons delimiting the occurrence records in niche space were constructed using all records, but to aid visual presentation, only a random subset of 120 *L. dentata* occurrence records (equal to the number of *L. dayi* records) is shown.

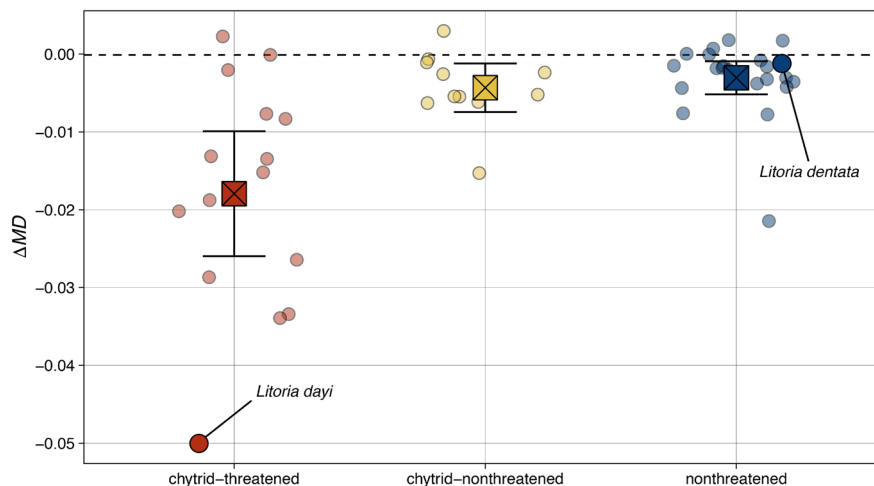


Figure 3. Change in the average Mahalanobis distance to the niche centroid for post-chytrid occurrence records relative to that for all occurrence records (ΔMD) for species in each of the three groups. Each species is shown as a filled circle with filled squares showing the average ΔMD for each group with bars representing 95% confidence intervals. Negative ΔMD values indicate that, on average, post-chytrid records are closer to the full niche centroid (contraction to the niche core), while positive values indicate the opposite (contraction to the niche margin). Chytrid-threatened species show a stronger tendency to contract toward the niche core relative to chytrid-nonthreatened and nonthreatened species.

distance values for the full set of records and the post-chytrid occurrence records. The first species, the Australian lace-lid *Litoria dayi*, is a chytrid-threatened species that has experienced severe realized niche contractions. These contractions are associated with a dramatic reduction in the average Mahalanobis distance of post-chytrid occurrence records relative to the full records, reflecting contraction to the niche core. The second species, the bleating tree frog *L. dentata*, is a nonthreatened species that shows niche stability, with no substantial difference in the average Mahalanobis distance to the full niche centroid for post-chytrid occurrence records.

The average change in Mahalanobis distance post-chytrid (ΔMD) differed significantly between species groups ($\chi^2_{\text{Kruskal-Wallis}} = 13.30$, $p = 0.001$). Chytrid-threatened species had significantly lower ΔMD values (greater contraction to the niche core) than nonthreatened species (post hoc Dunn's test, $p < 0.001$; Fig. 3). Chytrid-threatened species also had lower ΔMD than chytrid-nonthreatened species, although the difference in ΔMD was smaller than the difference between chytrid-threatened and nonthreatened species (Fig. 3) and only marginally significant ($p = 0.05$). For chytrid-threatened species, ΔMD values were negative, indicating contraction toward the niche core, apart for two species. The chytrid-threatened Baw Baw frog *Philoria frosti* had slightly positive ΔMD , indicating a tendency to contract toward niche margins, and the southern corroboree frog *Pseudophryne corroboree* experienced little change in average ΔMD (Supporting information).

We compared the uniformity of niche contraction among species groups by locating occurrence records in a common 2D environmental space in which the post-chytrid niche centroid was always to the right of the full niche centroid (Fig. 1). Estimating the probability of persistence across

this 2D niche space using logistic regression confirmed that chytrid-threatened species tended to contract away from the margin and toward the core of their niches (Fig. 4). Species in the chytrid-nonthreatened and nonthreatened groups had higher probabilities of persistence across the 2D niche space, with less marked contraction from their niche margins (Fig. 4). Contractions were non-uniform for both chytrid-threatened and chytrid-nonthreatened species, evident as a higher probability of persistence at some niche margins relative to others (Fig. 4).

Discussion

Understanding patterns of species niche contraction can reveal pathways of decline and the role of environmental conditions in moderating threat impacts (Scheele et al. 2017a, Lomolino 2023). We show that declining Australian frog species impacted by an invasive pathogen, chytrid fungus, have generally contracted toward the core of their realized niches, not the margins. We also document a general pattern of non-uniform loss of niche space, with species contracting from some niche margins more so than others. This pattern of decline most likely arises because host performance declines while pathogen performance increases at the niche margins of the Australian frog species examined here.

The distributions of the frog species we studied completely overlap with the extent of chytrid fungus in eastern Australia (Murray et al. 2011, Sopniewski et al. 2022). However, it has been well documented that the impact of chytrid fungus on amphibians – in terms of virulence and population-level declines – is strongly environmentally mediated, both in Australia and elsewhere (Puschendorf et al. 2011, 2013,

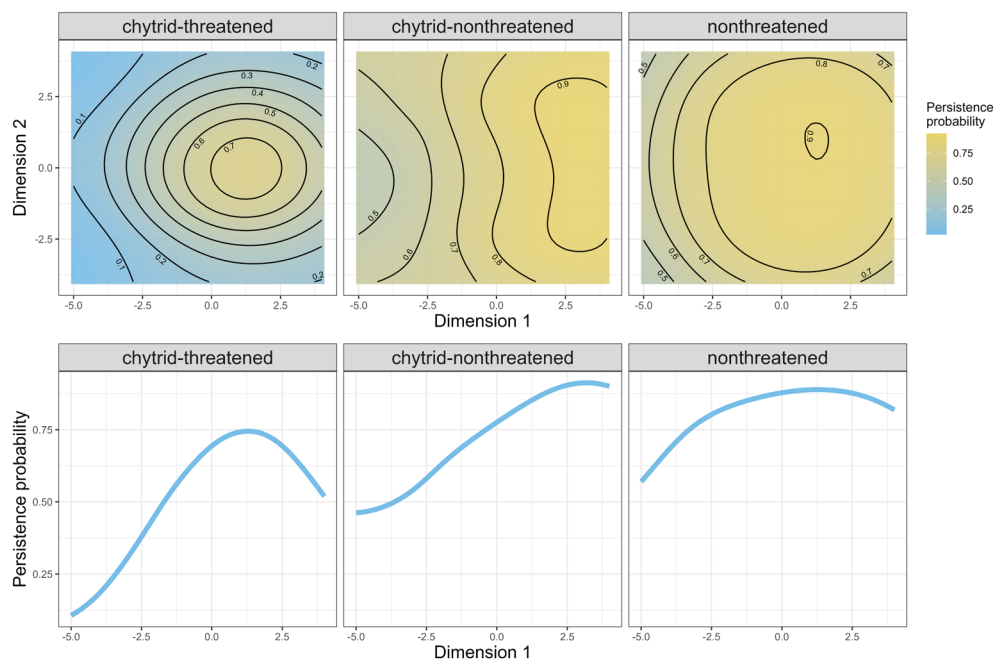


Figure 4. The average probability of persistence post-chytrid across the standardized 2D niche space for chytrid-threatened, chytrid-nonthreatened and nonthreatened species of Australian frogs. The standardized niche space is a 2D representation of the six pairwise combinations of four environmental variables (annual mean temperature, mean diurnal temperature range, annual precipitation and elevation). The variable combinations were stacked using the method shown in Fig. 1. In the top row, Dimension 1 and Dimension 2 are x and y axes, respectively, that map occurrence records for each pairwise combination of the four environmental variables onto a niche space with standardized centroid locations (Fig. 1). These contour plots and colors show the average probability of persistence across the standardized 2D niche space for each species group. In the bottom row, lines show the average probability of persistence for each species group across the first dimension only, holding the second dimension at its mean. Contraction to the niche core is indicated by higher probability of persistence toward the center of the standardized niche space (mean of each dimension) and lower probability of persistence toward the margins. Non-uniformity in niche contraction is evidenced by asymmetrical patterns across dimensions.

Heard et al. 2014, 2015, 2024, Fisher and Garner 2020, Brannelly et al. 2021, Scheele et al. 2024a). Among our focal species, those that have been severely impacted and are listed as threatened (chytrid-threatened species) tended to contract away from cooler, high elevation areas and areas with lower precipitation and greater temperature variability (Scheele et al. 2023, Fig. 2). These areas are thought to be more favourable to the pathogen and/or less optimal for frog population growth. For example, prevalence and virulence of chytrid fungus is closely tied to temperature in Australia (Sopniewski et al. 2022, Scheele et al. 2023), with cooler temperatures within the typical range for eastern Australia tending to favour the pathogen (Piotrowski et al. 2004, Sheets et al. 2021). This helps explain contractions of frog species away from cooler regions and higher elevations. However, these factors also influence the ability of frog hosts to tolerate increased mortality. Frogs in cooler and higher elevation areas have reduced growth rates and longer maturation times, with lower rates of population growth (Scheele et al. 2024a). Similarly, contractions away from drier areas with greater temperature variability are likely related to the impact of these conditions on frog population growth rates. In such environments, frogs experience lower and more erratic recruitment and higher adult mortality (Morrison and Hero

2003, Caruso and Rissler 2019). Hence, the observed contraction to the niche core among Australian frogs impacted by chytrid likely results from the interplay between environmental drivers of both pathogen virulence and host resilience.

Temperature appears particularly important in this regard, in line with the ‘thermal mismatch hypothesis’ (Nowakowski et al. 2016, Cohen et al. 2017). The thermal mismatch hypothesis posits that individual and population-level performance of hosts and pathogens across temperature gradients is a fundamental determinant of pathogen impacts, with hosts being less susceptible to pathogens in environments closer to the thermal optima of the host (Cohen et al. 2017) or those with temperature regimes that are more tolerable to hosts than to pathogens (Nowakowski et al. 2016). As both mean annual temperature and diurnal temperature range are key characteristics of the niche shifts documented here (Fig. 2; Scheele et al. 2023), we suggest thermal mismatches are likely to be a key underlying mechanism determining population extinctions and persistence for susceptible frog species in Australia. Testing this requires information on the relative performance of frogs and chytrid fungus across the thermal axes of the realized niche space of frogs. While challenging, such studies would provide vital insights into host–pathogen dynamics and useful guidance for conservation

actions, such as small-scale interventions that can support host performance in areas otherwise highly suitable for the pathogen (Scheele et al. 2014).

Contraction to the core was not a universal outcome for Australian frogs impacted by chytrid fungus. Some species included in our study displayed minimal change in Mahalanobis distances and one (the Baw Baw frog *Philoria frosti*) displayed a positive ΔMD suggesting ecological marginalization since chytrid emergence (Fig. 3). Evidence of ecological marginalization is also available for another Australian frog that has been severely impacted by chytrid fungus, but which could not be included in our analysis due to a lack of sufficient records. The armoured mistfrog *Litoria lorica* was formerly considered restricted to rocky rainforest streams and feared extinct when all known populations were extirpated after chytrid emerged. However, a remnant population was rediscovered and persists along a rocky stream in open woodland habitat characterized by drier, warmer conditions with high insolation, where chytrid virulence is reduced (Puschendorf et al. 2011). The extremely restricted range of the species at this remnant site (< 2 km of stream) suggests that the conditions are marginal for the species, with persistence likely due to the similarly marginal nature of these conditions for the pathogen.

The example of the armoured mistfrog is also useful for highlighting the role of microscale conditions in macroscale niche shifts. For this species, warm rock faces and crevices appear crucial for raising body temperatures to sufficient levels to mitigate infection intensity (Puschendorf et al. 2011). Thermal refuges at both microhabitat- and wetland-levels are known among amphibians in the Northern Hemisphere (e.g. for the Mallorcan midwife toad *Alytes muletensis*; Doddington et al. 2013), and our own work has identified them for two other species of Australian hylids (Heard et al. 2015, Clulow et al. 2018). While our analyses focused on macroclimate conditions, these examples demonstrate that variation in microclimate conditions within areas broadly suitable for chytrid fungus can inhibit pathogen impacts, potentially shaping patterns of population decline at macroscales. It is possible, for example, that a lack of niche shifts at macroscales could mask the exclusion of species from cool microhabitats that were previously occupied. Likewise, the degree of microscale environmental variation could itself be a mechanism for macroscale shifts. For example, it is possible that retraction to the core at the macroscale occurs because there is greater microclimatic variation for hosts at the niche core, providing more opportunities for thermal mismatch with the pathogen (Nowakowski et al. 2016, Cohen et al. 2017).

Our standardization procedure enabled us to assess whether niche contractions post-chytrid occurred uniformly or non-uniformly across niche space. Observing the pattern of persistence across the first dimension in Fig. 4 (bottom panel), chytrid-nonthreatened species exhibit a somewhat linear decline right to left, whereas chytrid-threatened species show a humped response right to left. We interpret these results to indicate that while species in both groups

experienced declines due to chytrid's emergence, declines for chytrid-nonthreatened species tended to be less uniform and concentrated toward one margin of their niche space. In contrast, chytrid-threatened species underwent more severe declines overall, with more uniform losses around their niche margins. The greater magnitude and uniformity of contractions in the chytrid-threatened group align with these species declining to such an extent that they are now recognized as threatened. For example, while the green and golden bell frog *Litoria aurea* experienced more severe declines at high elevations, numerous populations have also been lost in coastal, lowland areas that serve as refugia for this species (Mahony et al. 2013, Clulow et al. 2018). In contrast, the chytrid-impacted, but non-threatened Bibron's toadlet *Pseudophryne bibronii* has declined from the higher elevation parts of its niche, but lowland populations are apparently stable and unaffected (Scheele et al. 2017b). Hence, while the general patterns of decline are similar between these two species, the extent of environmental mediation of both pathogen virulence and host resilience varies greatly.

Understanding changes in the niche characteristics of declining species holds much promise for both better understanding the drivers of variable patterns of decline, and for guiding the development of effective conservation responses (Scheele et al. 2017a, Lomolino 2023). However, identifying common patterns of decline across all species is likely to be challenging, as threatening processes impact species in diverse ways, with these impacts moderated by the degree of threat overlap, underlying environmental conditions, and species biology (Isaac and Cowlshaw 2004, Cowlshaw et al. 2009, Scheele et al. 2017a). Our finding that most pathogen-impacted frogs have generally contracted toward their niche core contrasts with the pattern of ecological marginalization in a global analysis of declining mammals, for which habitat loss, habitat degradation and over-exploitation are key threats (Britnell et al. 2023). Taken together, our results and those of Britnell et al. (2023) suggest there can be commonalities in the patterns of niche change among groups of species impacted by a common threatening process. We encourage further cross-taxa studies on patterns of niche shifts among declining species, with a focus on elucidating the underlying mechanisms that give rise to both the commonalities and idiosyncrasies of niche contractions. Analyses that examine different aspects of niche shifts, such as those presented here, will help by quantifying the amount of niche breadth lost, and the directionality and uniformity of niche contractions, providing insight into both when and how particular threatening processes drive contractions toward the niche core or margins.

Acknowledgements – FrogID data were used with the permission of the Australian Museum. We thank Jodi Rowley for enabling access to these data, and Marcel Cardillo, Conrad Hoskin, Graeme Gillespie, Michael Mahony, David Newell and Jodi Rowley for assistance with record vetting and helpful discussions.

Funding – BCS was supported by The Australian Research Council through a Discovery Early Career Research Award (DE200100121).

Author contributions

Ben C. Scheele: Conceptualization (equal); Data curation (supporting); Formal analysis (supporting); Funding acquisition (lead); Investigation (lead); Methodology (supporting); Project administration (lead); Visualization (supporting); Writing – original draft (lead); Writing – review and editing (lead). **Geoffrey W. Heard:** Conceptualization (supporting); Formal analysis (supporting); Investigation (equal); Methodology (supporting); Visualization (supporting); Writing – original draft (supporting); Writing – review and editing (supporting). **Richard P. Duncan:** Conceptualization (supporting); Investigation (supporting); Methodology (supporting); Writing – original draft (supporting); Writing – review and editing (supporting). **Simon Clulow:** Investigation (supporting); Visualization (supporting); Writing – original draft (supporting); Writing – review and editing (supporting). **Jarrod Sopniewski:** Conceptualization (equal); Data curation (lead); Formal analysis (lead); Investigation (supporting); Methodology (equal); Visualization (lead); Writing – original draft (supporting); Writing – review and editing (supporting).

Transparent peer review

The peer review history for this article is available at <https://www.webofscience.com/api/gateway/wos/peer-review/10.1111/ecog.07612>.

Data availability statement

Data are available from the Zenodo Archive: <https://zenodo.org/records/14020777> (Scheele et al. 2024b).

Supporting information

The Supporting information associated with this article is available with the online version.

References

- Blonder, B., Lamanna, C., Violle, C. and Enquist, B. J. 2014. The n -dimensional hypervolume. – *Global Ecol. Biogeogr.* 23: 595–609.
- Blonder, B., Morrow, C. B., Maitner, B., Harris, D. J., Lamanna, C., Violle, C., Enquist, B. J. and Kerkhoff, A. J. 2018. New approaches for delineating n -dimensional hypervolumes. – *Methods Ecol. Evol.* 9: 305–319.
- Bogoni, J. A., Ferraz, K. M. P. M. B. and Peres, C. A. 2022. Continental-scale local extinctions in mammal assemblages are synergistically induced by habitat loss and hunting pressure. – *Biol. Conserv.* 272: 109635.
- Brannelly, L. A., McCallum, H. I., Grogan, L. F., Briggs, C. J., Ribas, M. P., Hollanders, M., Sasso, T., Familiar López, M., Newell, D. A. and Kilpatrick, A. M. 2021. Mechanisms underlying host persistence following amphibian disease emergence determine appropriate management strategies. – *Ecol. Lett.* 24: 130–148.
- Britnell, J. A., Zhu, Y., Kerley, G. I. H. and Shultz, S. 2023. Ecological marginalization is widespread and increases extinction risk in mammals. – *Proc. Natl Acad. Sci. USA* 120: e2205315120.
- Broennimann, O., Petitpierre, B., Chevalier, M., González-Suárez, M., Jeschke, J. M., Rolland, J., Gray, S. M., Bacher, S. and Guisan, A. 2021. Distance to native climatic niche margins explains establishment success of alien mammals. – *Nat. Commun.* 12: 2353. <https://doi.org/10.1038/s41467-021-22693-0>.
- Caruso, N. M. and Rissler, L. J. 2019. Demographic consequences of climate variation along an elevational gradient for a montane terrestrial salamander. – *Popul. Ecol.* 61: 171–182.
- Channell, R. and Lomolino, M. V. 2000a. Dynamic biogeography and conservation of endangered species. – *Nature* 403: 84–86.
- Channell, R. and Lomolino, M. V. 2000b. Trajectories to extinction: spatial dynamics of the contraction of geographical ranges. – *J. Biogeogr.* 27: 169–179.
- Clulow, S., Gould, J., James, H., Stockwell, M., Clulow, J. and Mahony, M. 2018. Elevated salinity blocks pathogen transmission and improves host survival from the global amphibian chytrid pandemic: implications for translocations. – *J. Appl. Ecol.* 55: 830–840.
- Cohen, J. M., Venesky, M. D., Sauer, E. L., Civitello, D. J., McMahon, T. A., Roznik, E. A. and Rohr, J. R. 2017. The thermal mismatch hypothesis explains host susceptibility to an emerging infectious disease. – *Ecol. Lett.* 20: 184–193.
- Colwell, R. K. and Rangel, T. F. 2009. Hutchinson's duality: the once and future niche. – *Proc. Natl Acad. Sci. USA* 106: 19651–19658.
- Cowlishaw, G., Pettifor, R. A. and Isaac, N. J. 2009. High variability in patterns of population decline: the importance of local processes in species extinctions. – *Proc. R. Soc. B* 276: 63–69.
- Doddington, B. J., Bosch, J., Oliver, J. A., Grassly, N. C., Garcia, G., Schmidt, B. R., Garner, T. W. J. and Fisher, M. C. 2013. Context-dependent amphibian host population response to an invading pathogen. – *Ecology* 94: 1795–1804.
- Doherty, T. S., Glen, A. S., Nimmo, D. G., Ritchie, E. G. and Dickman, C. R. 2016. Invasive predators and global biodiversity loss. – *Proc. Natl Acad. Sci. USA* 113: 11261–11265.
- Duong, T. 2007. ks: kernel density estimation and kernel discriminant analysis for multivariate data in R. – *J. Stat. Softw.* 21: 1–16.
- Eberhard, E. K., Wilcove, D. S. and Dobson, A. P. 2022. Too few, too late: US Endangered Species Act undermined by inaction and inadequate funding. – *PLoS One* 17: e0275322.
- Fick, S. E. and Hijmans, R. J. 2017. WorldClim 2: new 1-km spatial resolution climate surfaces for global land areas. – *Int. J. Climatol.* 37: 4302–4315.
- Fisher, D. O. 2011. Trajectories from extinction: where are missing mammals rediscovered? – *Global Ecol. Biogeogr.* 20: 415–425.
- Fisher, M. C. and Garner, T. W. J. 2020. Chytrid fungi and global amphibian declines. – *Nat. Rev. Microbiol.* 18: 332–343.
- Fristoe, T. S., Vilela, B., Brown, J. H. and Botero, C. A. 2023. Abundant-core thinking clarifies exceptions to the abundant-center distribution pattern. – *Ecography* 2023: e06365.
- Gillespie, G. R., Roberts, J. D., Hunter, D., Hoskin, C. J., Alford, R. A., Heard, G. W., Hines, H., Lemckert, F., Newell, D. and Scheele, B. C. 2020. Status and priority conservation actions for Australian frog species. – *Biol. Conserv.* 247: 108543.
- Guisan, A., Petitpierre, B., Broennimann, O., Daehler, C. and Kueffer, C. 2014. Unifying niche shift studies: insights from biological invasions. – *Trends Ecol. Evol.* 29: 260–269.

- Heard, G. W., Scroggie, M. P., Clemann, N. and Ramsey, D. S. L. 2014. Wetland characteristics influence disease risk for a threatened amphibian. – *Ecol. Appl.* 24: 650–662.
- Heard, G. W., Thomas, C. D., Hodgson, J. A., Scroggie, M. P., Ramsey, D. S. and Clemann, N. 2015. Refugia and connectivity sustain amphibian metapopulations afflicted by disease. – *Ecol. Lett.* 18: 853–863.
- Heard, G., Scroggie, M., Hollanders, M. and Scheele, B. C. 2024. Age truncation due to disease shrinks metapopulation viability for amphibians. – *J. Anim. Ecol.* 93: 1670–1683.
- Hengeveld, R. and Haeck, J. 1982. The distribution of abundance. I. Measurements. – *J. Biogeogr.* 9: 303–316. <https://doi.org/10.2307/2844717>
- Hijmans, R. J., Bivand, R., Forner, K., Ooms, J., Pebesma, E. and Sumner, M. D. 2022. – <https://rspatial.github.io/terra/>.
- IPBES 2019. Global assessment report on biodiversity and ecosystem services of the intergovernmental science-policy platform on biodiversity and ecosystem services. – IPBES Secretariat.
- Isaac, N. J. and Cowlshaw, G. 2004. How species respond to multiple extinction threats. – *Proc. R. Soc. B* 271: 1135–1141.
- Karger, D. N., Nobis, M. P., Normand, S., Graham, C. H. and Zimmermann, N. E. 2023. CHELSA-TraCE21k–high-resolution (1 km) downscaled transient temperature and precipitation data since the last glacial maximum. – *Clim. Past* 19: 439–456.
- Lomolino, M. V. 2023. The ecological and geographic dynamics of extinction: niche modeling and ecological marginalization. – *Proc. Natl Acad. Sci. USA* 120: e2220467120.
- Lomolino, M. V. and Channell, R. 1995. Splendid isolation: patterns of geographic range collapse in endangered mammals. – *J. Mammal.* 76: 335–347.
- Luedtke, J. A. et al. 2023. Ongoing declines for the world's amphibians in the face of emerging threats. – *Nature* 622: 308–314.
- Mahony, M. J., Hamer, A. J., Pickett, E. J., McKenzie, D. J., Stockwell, M. P., Garnham, J. I., Keely, C. C., Deboo, M. L., O'Meara, J., Pollard, C. J. and Clulow, S. 2013. Identifying conservation and research priorities in the face of uncertainty: a review of the threatened bell frog complex in eastern Australia. – *Herpetol. Conserv. Biol.* 8: 519–538.
- Martínez-Meyer, E., Díaz-Porrás, D., Peterson, A. T. and Yáñez-Arenas, C. 2013. Ecological niche structure and rangewide abundance patterns of species. – *Biol. Lett.* 9: 20120637.
- Maxwell, S. L., Fuller, R. A., Brooks, T. M. and Watson, J. E. 2016. Biodiversity: the ravages of guns, nets and bulldozers. – *Nature* 536: 143–145.
- Morrison, C. and Hero, J. M. 2003. Geographic variation in life-history characteristics of amphibians: a review. – *J. Anim. Ecol.* 72: 270–279.
- Murray, K. A., Retallick, R. W. R., Puschendorf, R., Skerratt, L. F., Rosauer, D., McCallum, H. I., Berger, L., Speare, R. and VanDerWal, J. 2011. Assessing spatial patterns of disease risk to biodiversity: implications for the management of the amphibian pathogen, *Batrachochytrium dendrobatidis*. – *J. Appl. Ecol.* 48: 163–173.
- Naimi, B., Hamm, N. A. S., Groen, T. A., Skidmore, A. K. and Toxopeus, A. G. 2014. Where is positional uncertainty a problem for species distribution modelling? – *Ecography* 37: 191–203.
- Nowakowski, A. J., Whitfield, S. M., Eskew, E. A., Thompson, M. E., Rose, J. P., Caraballo, B. L., Kerby, J. L., Donnelly, M. A. and Todd, B. D. 2016. Infection risk decreases with increasing mismatch in host and pathogen environmental tolerances. – *Ecol. Lett.* 19: 1051–1061.
- Osorio-Olvera, L., Soberón, J. and Falconi, M. 2019. On population abundance and niche structure. – *Ecography* 42: 1415–1425.
- Osorio-Olvera, L., Yáñez-Arenas, C., Martínez-Meyer, E. and Peterson, A. T. 2020. Relationships between population densities and niche-centroid distances in North American birds. – *Ecol. Lett.* 23: 555–564.
- Peterson, A. T., Soberón, J., Pearson, R. G., Anderson, R. P., Martínez-Meyer, E. and Nakamura, M. 2011. Ecological niches and geographic distributions. – Princeton Univ. Press.
- Piotrowski, J. S., Annis, S. L. and Longcore, J. E. 2004. Physiology of *Batrachochytrium dendrobatidis*, a chytrid pathogen of amphibians. – *Mycologia* 96: 9–15.
- Pironon, S., Papuga, G., Vilellas, J., Angert, A. L., García, M. B. and Thompson, J. D. 2017. Geographic variation in genetic and demographic performance: new insights from an old biogeographical paradigm. – *Biol. Rev.* 92: 1877–1909.
- Puschendorf, R., Hoskin, C. J., Cashins, S. D., McDonald, K., Skerratt, L. F., VanDerWal, J. and Alford, R. A. 2011. Environmental refuge from disease-driven amphibian extinction. – *Conserv. Biol.* 25: 956–964.
- Puschendorf, R., Hodgson, L., Alford, R. A., Skerratt, L. F. and VanDerWal, J. 2013. Underestimated ranges and overlooked refuges from amphibian chytridiomycosis. – *Divers. Distrib.* 19: 1313–1321.
- Richardson, D. M. and Whittaker, R. J. 2010. Conservation biogeography—foundations, concepts and challenges. – *Divers. Distrib.* 16: 313–320.
- Scheele, B. C., Hunter, D. A., Grogan, L., Berger, L., Kolby, J. E., McFadden, M. S., Marantelli, G., Skerratt, L. F. and Driscoll, D. A. 2014. Interventions for reducing extinction risk in chytridiomycosis-threatened amphibians. – *Conserv. Biol.* 28: 1195–1205.
- Scheele, B. C., Foster, C. N., Banks, S. C. and Lindenmayer, D. B. 2017a. Niche contractions in declining species: mechanisms and consequences. – *Trends Ecol. Evol.* 32: 346–355.
- Scheele, B. C., Skerratt, L. F., Grogan, L. F., Hunter, D. A., Clemann, N., McFadden, M., Newell, D., Hoskin, C. J., Gillespie, G. R., Heard, G. W., Brannelly, L., Roberts, A. A. and Berger, L. 2017b. After the epidemic: ongoing declines, stabilizations and recoveries in amphibians afflicted by chytridiomycosis. – *Biol. Conserv.* 206: 37–46.
- Scheele, B. C., Foster, C. N., Hunter, D. A., Lindenmayer, D. B., Schmidt, B. R. and Heard, G. W. 2019a. Living with the enemy: facilitating amphibian coexistence with disease. – *Biol. Conserv.* 236: 52–59.
- Scheele, B. C. et al. 2019b. Amphibian fungal panzootic causes catastrophic and ongoing loss of biodiversity. – *Science* 363: 1459–1463.
- Scheele, B. C., Heard, G. W., Cardillo, M., Duncan, R. P., Gillespie, G. R., Hoskin, C. J., Mahony, M., Newell, D., Rowley, J. J. L. and Sopniewski, J. 2023. An invasive pathogen drives directional niche contractions in amphibians. – *Nat. Ecol. Evol.* 7: 1682–1692.
- Scheele, B. C., Webb, R. J., Hua, X. and Hollanders, M. 2024a. Variation in amphibian maturation rates influences population vulnerability to disease-induced declines. – *Anim. Conserv.* 27: 600–610.
- Scheele, B. C., Heard, G. W., Duncan, R. P., Clulow, S. and Sopniewski, J. 2024b. Data from: An invasive pathogen generally contracts species to their niche cores, not margins. – Zenodo Archive, <https://zenodo.org/records/14020777>.
- Sheets, C. N., Schmidt, D. R., Hurtado, P. J., Byrne, A. Q., Rosenblum, E. B., Richards-Zawacki, C. L. and Voyles, J. 2021.

- Thermal performance curves of multiple isolates of *Batrachochytrium dendrobatidis*, a lethal pathogen of amphibians. – *Front. Vet. Sci.* 8: 687084.
- Sopniewski, J., Scheele, B. C. and Cardillo, M. 2022. Predicting the distribution of Australian frogs and their overlap with *Batrachochytrium dendrobatidis* under climate change. – *Divers. Distrib.* 28: 1255–1268.
- Watson, D. M. 2011. A productivity-based explanation for woodland bird declines: poorer soils yield less food. – *Emu Austral Ornithol.* 111: 10–18.
- Wintle, B. A., Cadenhead, N. C., Morgain, R. A., Legge, S. M., Bekessy, S. A., Cantele, M., Possingham, H. P., Watson, J. E. M., Maron, M., Keith, D. A., Garnett, S. T., Woinarski, J. C. Z. and Lindenmayer, D. B. 2019. Spending to save: what will it cost to halt Australia's extinction crisis? – *Conserv. Lett.* 12: e12682.
- Yamaura, Y., Amano, T., Kusumoto, Y., Nagata, H. and Okabe, K. 2011. Climate and topography drives macroscale biodiversity through land-use change in a human-dominated world. – *Oikos* 120: 427–451.